Biol. Stud. 2025, 19(3), 3–20 • doi: https://doi.org/10.30970/sbi.1903.837
www.http://publications.lnu.edu.ua/journals/index.php/biology

UDC: 577.33

DETECTION OF ALKALINE PHOSPHATASE ACTIVITY IN BLOOD SERUM USING A RECOMBINATION-BASED SEMICONDUCTOR SENSOR

Sergii Litvinenko **, *Oleksii Kozinetz*** **, *Bogdan Sus*** **, *Olga Tsymbalyuk*** **

Taras Shevchenko National University of Kyiv, 64/13 Volodymyrska St., Kyiv 01601, Ukraine

Litvinenko, S., Kozinetz, O., Sus, B., & Tsymbalyuk, O. (2025). Detection of alkaline phosphatase activity in blood serum using a recombination-based semiconductor sensor. *Studia Biologica*, 19(3), 3–20. doi:10.30970/sbi.1903.837

Background. Most pathologies of the human body (malignant liver tumors, cholestasis, preeclampsia, gestational diabetes, prostate cancer, etc.) are accompanied by a violation of the integrity of cells in target tissues and the release of intracellular macromolecules into the extracellular environment. Thus, an important diagnostic and prognostic indicator is the level of activity of certain enzymes, which are normally intracellular, in blood serum. One of the most promising areas of modern medical electronics and biophysics is the development and optimization of enzyme screening methods in biological fluids. In this study, we aimed to investigate the biophysical characteristics of alkaline phosphatase (ALP) using a recombination sensor for determining activity in biological fluids.

Materials and Methods. Experiments were performed on preparations of standard human blood serum. The reference determination of alkaline phosphatase activity was carried out photometrically. The passage of the alkaline phosphatase reaction was experimentally recorded by measuring the photocurrent of a silicon structure with a buried barrier under several additional factors, such as modified electric fields or modulated illumination.

Results. The biophysical features were studied. The detection of ALP becomes possible due to cleaving 4-nitrophenyl phosphate to phenol. These chemical reactions are accompanied by a redistribution of the reagent charges, particularly an increase in negative charge. The effect is explained by the local electrostatic influence on the parameters of the recombination centers near the silicon surface, which leads to a change in the surface recombination rate.

Conclusions. Our approach can be regarded as promising for the development of a highly sensitive method for the detection of ALP. It has been experimentally shown that effective detection is possible due to the rearrangement of electronic states at the SiO_x/Si interface of the deep barrier silicon following the adsorption.

Keywords: alkaline phosphatase, enzymatic activity, initial band bending, photoelectrical transducer, surface recombination velocity, biomedical diagnostic

INTRODUCTION

Biochemical markers of physiological conditions are among the most widely used diagnostic indicators. Their determination is crucial for screening the health status of individuals. Measurement of enzyme activity levels in blood serum and other biological fluids provides for monitoring the onset of pathological processes and predicting the degree of dysfunction in specific organs. Alkaline phosphatase (ALP) is one of the key marker enzymes. Its serum activity is included in the list of recommended routine examinations of the general condition of the body and checking the initial stages of development of pathologies of the cardiovascular and hepatobiliary systems and oncogenesis (Zhang *et al*., 2021; Shaban *et al*., 2022; Jiang *et al*., 2023). An elevated ALP activity level in blood serum is most commonly observed in liver damage. This enzyme, along with alanine and aspartate transaminases and bilirubin, serves as a marker for cholestasis (Su *et al*., 2022; Atia *et al*., 2024). An increase in ALP levels is most commonly associated with extensive hepatocyte destruction in hepatitis of various etiologies and malignant liver tumors. Prostate cancer has a greater tendency to metastasize to the bones compared to other malignancies. Regular monitoring of ALP levels in such patients enables early detection of potential bone metastases and their subsequent treatment (Jiang *et al*., 2023). Elevated serum ALP activity can also be linked to disrupted bone tissue function due to an increased osteoblast activity in conditions such as bone tumors, rickets, hyperparathyroidism, osteomalacia, and fractures. ALP is currently considered a key regulator of vascular calcification and, consequently, an important factor in the progression of cardiovascular diseases (Azpiazu *et al*., 2019; Brichacek *et al*., 2019). However, it is important to note that increased ALP activity levels in blood plasma can have normal physiological causes. Specifically, a progressive rise in this marker is observed during pregnancy (Li *et al*., 2023). A decrease in ALP activity in blood serum is also a significant diagnostic and prognostic indicator, which can be seen in certain pathologies, such as preeclampsia, gestational diabetes, and specific types of tumors, including colorectal and breast cancer (Xiao *et al*., 2019; Su *et al*., 2022; Jiang *et al*., 2023; Riancho, 2023). The term ALP generally refers to the catalysis of the hydrolysis of phosphate-containing esters at alkaline pH; however, this reaction is catalyzed by a family of enzymes with broad substrate specificity. These enzymes hydrolyze and transphosphorylate phosphate-containing esters (mainly phosphoethanolamine and pyridoxal-5′-phosphate) as well as pyrophosphate (PP_i) (Pabis & Kamerlin, 2016; Vimalraj, 2020). ALP molecules are homodimeric, membrane-associated glycoproteins, each containing three metal ions in the active site of each subunit: two Zn^{2+} ions and one Mg^{2+} ion. In humans, at least four forms of ALP are expressed: intestinal (characteristic of the intestinal epithelium, denoted as IALP), placental (characteristic of the placenta, denoted as PLALP), germ cell (characteristic of early embryonic cells, denoted as GALP), and a tissue-nonspecific

form, which is present in various tissues throughout the body (denoted as TNSALP or liver/bone/kidney ALP–L/B/K ALP) (Su *et al.*, 2022; Jiang *et al.*, 2023). In the human genome, the genes for the first three isoforms are located on chromosome 2, while the TNSALP isoforms are located on chromosome 1 (Millán & Whyt, 2016; Brichacek & Brown, 2019; Sato *et al*., 2021). Currently, the standard laboratory method for determining serum ALP activity, which is also used in automated biochemical analyzers, employs an indirect chemical method with photometric measurement of the reaction product. The first reaction involves the enzymatic hydrolysis of phenyl phosphate, while the second reaction occurs between the phenol produced by the enzyme and 4-phenylaminozin, resulting in the formation of a colored product, 4-nitrophenol (Young, 1997; Kaplan *et al*., 1996). However, this method has several limitations. First, even trace amounts of hemoglobin can interfere with the photometric measurement of the colored reaction product. Second, the method requires the use of alkaline reagents, which are potentially hazardous. Additionally, the enzymatic reaction produces phenol, a highly toxic substance (class 2 toxicity) that can enter the body through inhalation or skin contact, causing carcinogenesis and damage to the central nervous and cardiovascular systems (IARC, 1999; Nešvera *et al*., 2005). Furthermore, a 0.1% sodium azide is added to the reagent mixture for antimicrobial preservation, but sodium azide is a mutagen and belongs to the class of highly toxic and environmentally hazardous substances (Tat *et al*., 2021). Various pathological processes in the body, which are associated with an increased serum ALP activity, result from the presence of specific isoforms of phosphatase in the blood. Consequently, additional methodological approaches are employed in laboratory diagnostics to differentiate these isoforms when necessary. These methods include the use of selective isoenzyme inhibitors (e.g., urea, levamisole, L-phenylalanine, L-homoarginine, L-leucine), as well as electrophoretic protein separation techniques and affinity chromatography (Sharma *et al*., 2014; Villa-Suárez *et al*., 2021). Furthermore, although the TNSALP isoform shares complete identity in its primary structure, it undergoes distinct modifications via glycosylation, which leads to molecular differences in various tissues. This variation enables the differentiation of tissue origins in detailed blood serum studies. In this context, the simplest method to distinguish between liver and bone ALP is pre-heating the blood serum (Brichacek & Brown, 2019; Jiang *et al.*, 2023). The identification of ALP isoenzymes using methods such as electrophoresis and chromatography cannot be widely applied in clinical practice due to their low throughput. Electrochemical methods for determining ALP activity, including amperometric, potentiometric, and conductometric techniques, show promise due to several advantages, such as the absence of measurement errors when samples are contaminated with hemoglobin, the ability to detect the reaction in real-time with the potential for kinetic analysis, relatively low equipment cost, and compactness. Additionally, these methods enable sensitivity enhancement through chemical modification of the sensor surface and the use of modulating signals (Simão *et al.*, 2018; Balbaied & Moore, 2019; Si *et al.*, 2023). However, these methods exhibit significant drawbacks, such as the potential contamination of electrodes, which hinders their transport and complicates the measurement of real samples (Goud *et al.*, 2021). Furthermore, electrochemical sensors and biosensors for determining ALP activity currently exist only as laboratory prototypes and are not yet utilized in clinical analyses. Therefore, there is an objective need to develop methods for determining ALP activity that minimize the shortcomings of the currently used laboratory determination methods.

One promising approach involves the development of recombinational sensor structures, which present a viable and more efficient solution to these challenges by utilizing advanced semiconductor material properties and surface interactions. These structures have the potential to address the limitations of conventional methods, offering enhanced sensitivity and selectivity in detecting ALP activity. Furthermore, they can be engineered to specifically respond to target analytes, providing more precise and reliable alternatives to existing diagnostic techniques. The controlled and reproducible alteration of the recombinational characteristics of the semiconductor surface interface due to analyte adsorption underpins the operation of recombinational sensor structures. The photocurrent of the silicon structure with a deep junction energy barrier, measured under light illumination from the area of strong optical absorption, serves as a directly measurable parameter (Sato *et al*., 2021). These sensors exhibit high sensitivity to analytes containing molecules with intrinsic or induced dipole moments, while also offering relative simplicity in technological implementation. Therefore, it is reasonable to expect highly sensitive detection of metabolites with a pronounced dipole moment, particularly those produced by specific chemical reactions using recombinational sensor structures (Millán & Whyte, 2016). For optimal sensor performance, the photocurrent must be strongly influenced by changes in the surface recombination rate. The application of modulated illumination improves the sensor system's sensitivity by facilitating the amplification, processing, and extraction of relevant electronic signals from the background noise. Considering the intricate chemical processes associated with enzymatic reactions, it is essential to gather more reliable data on the analyte. To accomplish this task and to detect the fine structure of the signal, it may be beneficial to introduce supplementary influencing factors, such as constant voltage connection and continuous parametric light illumination (Kozynets *et al*., 2024).

The experimental logic was based on the premise that, upon contact between a liquid analyte and the surface of a semiconductor sensor, changes occur in the sensor's recombination characteristics and photocurrent, which are dependent on the analyte's properties. These changes are induced by the electrostatic interaction of the analyte molecules with the sensor's surface states, leading to alterations in the electron-hole recombination processes. The specificity of these changes is determined by the physicochemical properties of the analyte molecules, particularly their dipole moment and adsorption capacity on the sensor surface. Subsequent photocurrent measurements, under additional factors such as modified electric fields or modulated illumination, enable a more detailed detection and characterization of these changes. This facilitates the formation of a unique pattern for each analyte, which can be used for both identification and quantitative analysis. The primary objective of this study is to investigate these physical processes in detail and leverage them to develop novel analyte detection methods using semiconductor sensor structures.

MATERIALS AND METHODS

A structure with a deep *p*-*n*-junction barrier was used to investigate the adsorption processes, as shown in **Fig. 1*A***. The structures were fabricated on *p*-type silicon substrates with a resistivity of 50 Ω·cm. It was determined that the photocurrent of deep silicon barrier structure significantly depends on surface recombination when light with a high absorption coefficient is used (in other words, the area where light is absorbed and the space charge region should be spatially separated). For this reason, the thickness of

the base region *d* should be close to the diffusion length, whereas the silicon absorption coefficient $\alpha(\lambda)$ should be high (10^4–10^5 cm^{-1}) (Kozynets *et al*., 2024).

The crystal lattice orientation was (100). In the experiments, the sensor surface was illuminated by a green LED with a wavelength of λ = 550 nm and a nominal power of 10 mW. It operated with amplitude modulation at a frequency of 976 Hz, generating a principal photocurrent signal. The standard thickness *d* of silicon plates is 300 μm, which satisfies the requirements, as $d >> 1/\alpha(\lambda) \sim 0.07$ μm.

For additional illumination, a blue LED with a wavelength of λ = 470 nm and a power of 20 mW was used. The illumination intensity increased linearly to a maximum over 1 second, then decreased linearly. Simultaneously, a constant voltage was supplied across the liquid analyte, increasing linearly from 0 to 1500 mV over a period of 100 seconds.

The physical mechanism underlying the operation of the sensor can be explained within the framework of the Stevenson–Keyes theory, accounting for the simultaneous changes in the surface bending of energy bands, capture cross-sections, and the energetic position of recombination levels during adsorption. The supply of a constant voltage and parametric illumination should, in principle, produce a similar effect, influencing the band bending and carrier concentration in the surface area of the semiconductor sensor. The suggested scheme utilizes a relatively quick change in the intensity of parametric illumination against the background of a quasi-stationary change in constant voltage. It can be inferred that this approach will facilitate the detection of subtle variations in the amplitude of the photocurrent (for instance, changes associated with the reconstruction of recombination properties at the SiO_x/Si interface).

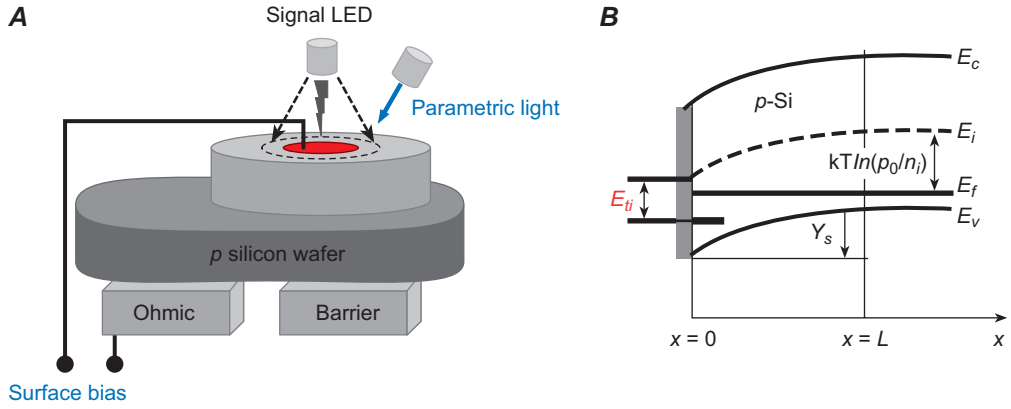

Fig. 1. ***A*** – diagram of the recombination semiconductor sensor, with the simultaneous parametric illumination and the supply of voltage, causing current to flow through the liquid analyte; ***B*** – energy band diagram of the *p*-Si semiconductor sensor structure's surface area

In the study, certified control samples of human blood serum lyophilisates PhiloNorm and PhiloPat were used, manufactured by "Filisit-Diagnostika", Ukraine. The reference determination of ALP activity in the serum samples was carried out by the scientific and production enterprise "Filisit-Diagnostika", Ukraine based on the reaction of cleavage of 4-nitrophenyl phosphate to phenol, followed by a reaction of phenol with 4-aminoantipyrine for photometric determination of the reaction product. It was found that the ALP activity in the Philonorm; serum sample was 398.4±6.7 IU/L (*n* = 7), and in the PhiloPat; sample it was 247.2±7.1 IU/L (*n* = 7).

The reference values of ALP activity in the blood serum of healthy adults are in the range of 40–190 IU/L, while in children and pregnant women, they can reach values over 500 IU/L. In the case of pathologies, the activity of this enzyme can be significantly increased (for example, in hepatitis) or decreased (for example, in hypothyroidism). With indicators of ALP activity in blood plasma less than 20 IU/L, an ALP deficiency state is diagnosed. Indicators of ALP activity in PhiloNorm and PhiloPat sera, which, in the case of spectroscopic determination by the reference method, agreed with the passport values of activity in the samples, correspond to the reference indicators for healthy adolescents under 18 years of age (Turan *et al*., 2011; Davis *et al*., 2024; Kalligosfyri *et al.*, 2025).

The assessment of ALP activity using a recombinant semiconductor sensor was performed by cleaving 4-nitrophenyl phosphate to phenol (**Fig. 2**). The reaction was induced by adding an aliquot of blood serum. The dissociation constants (pKa) of specific functional groups in the substrate and reaction product molecules were considered to evaluate the system's charge. The measurements were conducted under experimental conditions at pH 9.0 with an initial 4-nitrophenyl phosphate concentration of 0.01 M. At the initial stage, 1 mL of the reagent solution had a total negative charge of $5.4 \cdot 10^{20}$ elementary charges, determined by the partial dissociation of the phenolic and hydroxyl groups of 4-nitrophenyl phosphate at the given pH. After the reaction was completed, the system's charge increased to approximately $6.18 \cdot 10^{20}$ elementary charges per mL due to the dissociation of the reaction products, 4-nitrophenol and phosphoric acid. Thus, after the completion of the chemical reaction, the total negative charge in the system increases by 14.42 % ($7.78 \cdot 10^{19}$ charges), which is detected by the semiconductor sensor surface. This change in the effective charge of the reagents can influence the parameters of recombination centers at the interface, making it one of the key factors enabling the indirect detection of alkaline phosphatase activity. By considering the dissociation constants (pKa) of specific functional groups in the substrate and reaction product molecules, the system's charge can be evaluated under the experimental conditions used for reaction monitoring (pH 9.0, initial concentration of 4-nitrophenyl phosphate 0.01 M). Under these conditions, at the initial stage, 1 mL of the reagent solution exhibits a total negative charge of $5.4 \cdot 10^{20}$ elementary charges, arising from the presence of partially dissociated phenolic and hydroxyl groups of 4-nitrophenyl phosphate at this pH. Upon completion of the chemical reaction, the system acquires a significantly higher negative charge of approximately $6.18 \cdot 10^{20}$ elementary charges per mL, resulting from the dissociation of reaction product groups – 4-nitrophenol and phosphoric acid. Consequently, the total negative charge in the system increases by 14.42 % ($7.78 \cdot 10^{19}$ charges), which is detected by the semiconductor sensor surface. This change in the effective charge of the reagents, influencing the parameters of recombination centers at the interface, could be a key factor enabling the indirect detection of alkaline phosphatase activity.

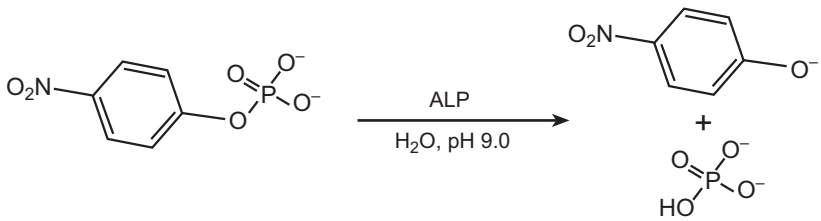

Fig. 2. Diagram of the reaction catalyzed by the enzyme alkaline phosphatase (ALP)

To assess the reproducibility of the obtained results, six experimental runs were performed, each comprising two measurements. In each case, the shape of the reference curve – reflecting the interaction of the sensor surface with the buffer and substrate – was examined prior to the introduction of PhiloPat and Philonorm. This curve remained virtually unchanged (as shown in **Figs 3*A*** and **3*B***, curve 2), thereby confirming the stability of the initial conditions. Only after this confirmation were the PhiloPat and PhiloNorm agents introduced, and the corresponding measurements subsequently performed. This protocol ensured consistency across all experimental runs. The accuracy of the photocurrent measurements was estimated to be within a few percent, which is considered acceptable for this type of analysis.

The enzyme activity in the PhiloPat preparation is reduced by one-third compared to that in Philonorm. Consequently, in the described reactions, a lower negative charge near the sensor surface is observed for PhiloPat while a higher charge is observed for Philonorm.

RESULTS AND DISCUSSION

A comparison of **Figs 3*A*** and **3*B*** reveals that when the semiconductor sensor surface is coated with only the buffer and substrate, the reference photocurrent curve remains nearly unchanged (curve 2). Therefore, for the initial analysis, the temporal variation of photocurrents should be assessed after the addition of the PhiloNorm and PhiloPat compounds (curve 1). In both cases, a negative charge is formed near the sensor surface, and the increase in photocurrent upon voltage supply is corresponded to by the transition of the near-surface area of the sensor from a state of maximum recombination rate, which is intrinsic conductivity, to a state of minimal recombination, which is inversion, as illustrated in **Fig. 1*A***. So, the key features that enable the distinction between PhiloNorm and PhiloPat in the experiment have been highlighted. When the adsorption of two liquid analytes results solely in a change in the near-surface bending of the energy bands (e.g., from Y_0 to Y_{S_1} and from Y_0 to Y_{S_2}), changes in the minimum and maximum photocurrent values can be expected upon application of a voltage sweep. This can be conceptualized as a shift in the photocurrent amplitude $i(Y)$ by the amount $Y_{S_1}–Y_{S_2}$. Although the precise relationship between the bending of the energy bands and the applied voltage is challenging to establish, the $i(Y)$ function would transition to a shifted version corresponding to a voltage shift of $\Delta V(Y_{S_1}–Y_{S_2})$. This effect is not observed in the series of experiments, at least not clearly: the maxima and minima of the photocurrent amplitude for both normal and pathological states coincide at the corresponding time points (**Figs 3*A***, **3*B***), which correspond to the moments when the minimum and maximum voltages are applied. Therefore, the adsorption of PhiloNorm and PhiloPat does not induce a significant difference between Y_{S_1} and Y_{S_2}. For intermediate voltage values, differences in the rate of photocurrent amplitude increase can be observed. This effect is likely associated with the rearrangement of electronic states at the SiO_x/Si interface following the adsorption of the liquid analyte. In **Fig. 3**, this is highlighted in red and blue.

We have applied the approaches developed in previous works (Tat *et al.*, 2021). It should be noted that the model parameters of the semiconductor sensor structure are as follows: charge carrier concentration in *p*-silicon wafer $p_0 = 10^{15}$ cm^{-3}, diffusion length l = 200 μm, silicon wafer thickness d = 250 μm, electron diffusion ratio D_n = 40 cm^2/s, charge carrier capture ratio at the surface level $c_n = c_p = 10^{-9}$ cm^{-2}, $N_t = 10^{11}$ cm^{-2} and

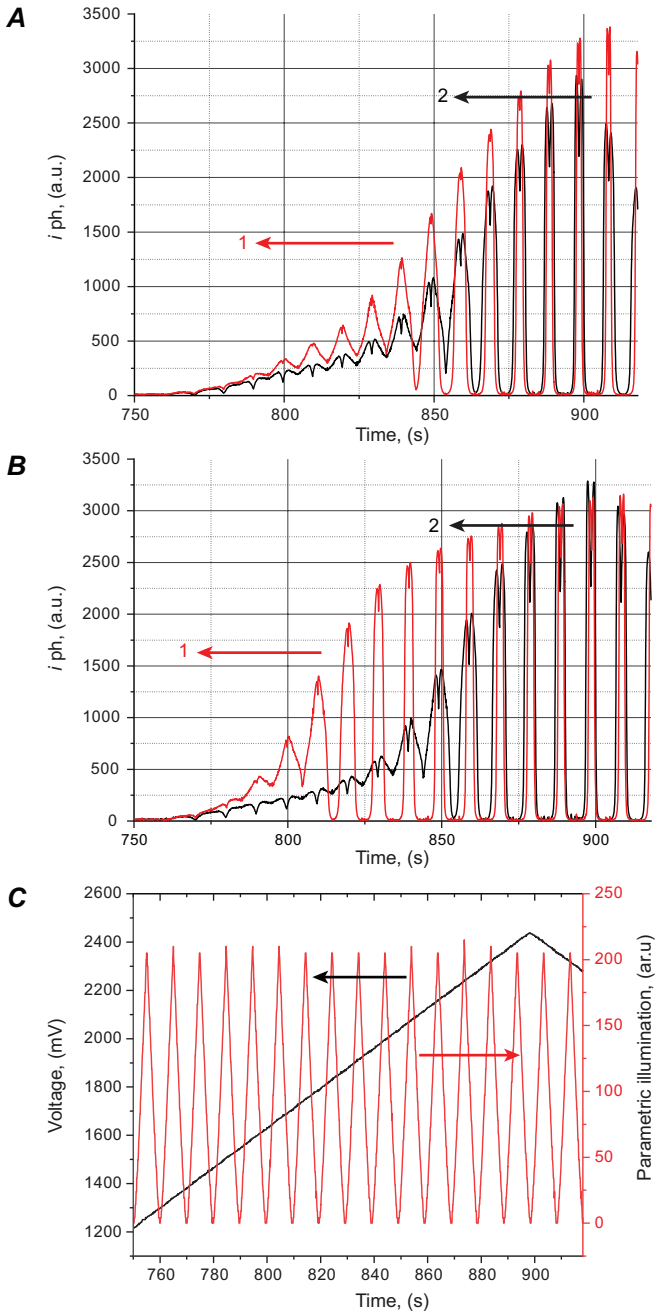

Fig. 3. ***A*** – dependence of photocurrent amplitude on time for different stages of the enzymatic chemical reaction for the case of pathological ALP activity in blood serum (curve 1 – PhiloPat and serum, curve 2 (reference) – buffer and substrate only); ***B*** – dependence of photocurrent amplitude on time for different stages of the enzymatic chemical reaction for normal ALP activity process in blood serum (curve1 – PhiloNorm and serum, curve 2 (reference) – buffer and substrate only). The graphs show the time-synchronized voltage sweep and parametric illumination; ***C*** – dependence of parametric illumination and surface voltage on time

energy E_{ti} = 0.1 kT counted from the middle of the silicon bandgap 1.12 eV, $n_i = 10^{11}$ cm^{-3} intrinsic concentration. It is important to note that in practice the levels whose energy was near the middle of the silicon bandgap determine recombination process at the interface. The recombination rate increases when the Fermi level gets close to the middle of the band gap. As for the decrease in recombination rate, the effect can be explained by the absence of carrier of a certain signal when the silicon surface is driven from the flat band through depletion into inversion condition. The further the level is from the middle bandgap (higher E_{ti}, see **Fig. 1*B***), the less contribution to the sensor signal is expected. The expression for recombination S at the semiconductor sensor interface is as follows:

$$S(Y_s) = \frac{c_p c_n N_t (p_0 + n_0)}{c_n \left(n_s(Y_s) + n_i \exp\left(\frac{E_{ti}}{\mathrm{kT}}\right)\right) + c_p \left(p_s(Y_s) + n_i \exp\left(\frac{E_{ti}}{\mathrm{kT}}\right)\right)}, \quad (1)$$

where $n_s = n_0 \exp(Y_s/\mathrm{kT})$, $p_s = p_0 \exp(-Y_s/\mathrm{kT})$, $n_0 = n_i^2/p_0$. The amplitude of the photocurrent (calculated at the edge x = L of space charge region), with the information about the progression of the chemical reaction over time, can be expressed as:

$$i(Y_s) \cong \frac{1 + \frac{s(Y)}{\alpha(\lambda) D}}{s(Y)\frac{l}{D}\mathrm{sh}\left(\frac{d}{l}\right) + \mathrm{ch}\left(\frac{d}{l}\right)}. \quad (2)$$

Let us examine in greater detail the potential for modifying the recombination parameters. A variation in E_{ti} influences S through an exponential dependence, as described in Equation (1). Numerical analysis suggests that this should result in a significant change in the photocurrent amplitude across the entire voltage range. **Fig. 4** presents the calculated photocurrent amplitude for different surface state concentrations N_t (curves 1–4, with N_t ranging from 10^{10} cm^{-2} to 10^{12} cm^{-2}). An increase in N_t leads to a symmetric broadening of the $i(Y)$ curve without altering its maximum or minimum values, as observed in **Fig. 4**. The analysis indicates that qualitative agreement with experimental data can be achieved under these conditions. It is reasonable to assume that a fraction of the centers becomes additionally involved in the recombination process. In other words, the analytes PhilorNorm and PhiloPat are expected to induce different concentrations of active recombination centers at the SiO_x/Si interface.

Another mechanism may involve a change in the charge carrier capture cross-sections due to the varying electrostatic influence on the recombination parameters at the interface. The analysis indicates that qualitative agreement with the experiment is also possible in this case. **Fig. 5** shows the results of photocurrent amplitude calculations for different capture cross-section ratios (c_n/c_p), with all other parameters held constant. It is noteworthy that the minimum of the photocurrent corresponds to different values of $Y_s = (\mathrm{kT}/2) \ln(c_p p_0/c_n n_0)$, in accordance with the condition $c_p p_s = c_n n_s$.

A correlation between experimental and theoretical data can be established if we assume that the analytes, during enzymatic reactions, modify the ratio of charge carrier capture cross-sections at the SiO_x/Si interface. It should be noted that, under these conditions, the energy band bending (Y_{S_1}) after the addition of PhiloNorm and the energy band bending (Y_{S_2}) after the addition of PhiloPat may be very similar. Nevertheless, our approach allows for the separate classification of these compounds. Based on these observations, the first characteristic for distinguishing the compounds is identified.

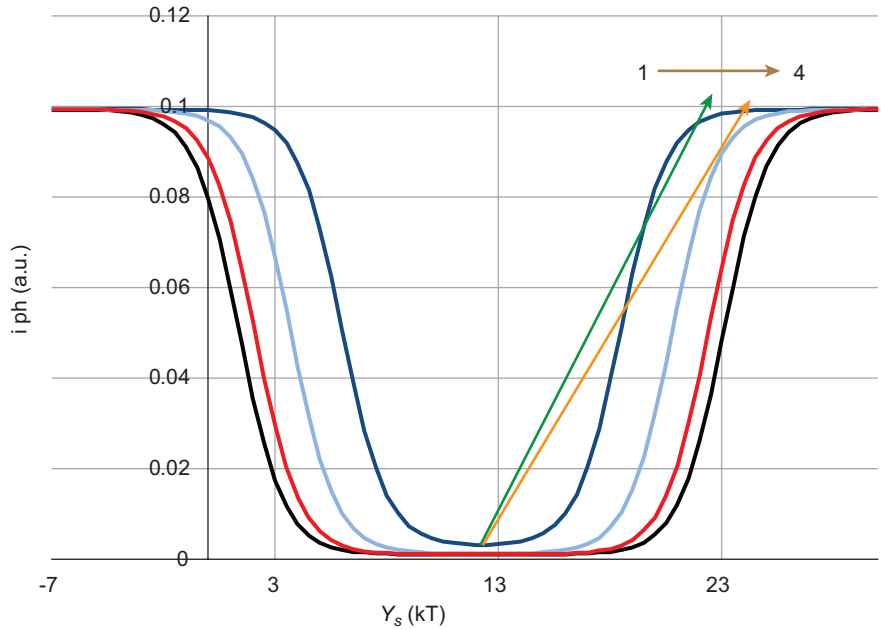

Fig. 4. Dependence of the photocurrent amplitude $i(Y_s)$ on the surface band bending for different concentrations of recombination centers: $N_t = 10^{10}$ 1/cm^2, $N_t = 5{\cdot}10^{10}$ 1/cm^2, $N_t = 10^{11}$ 1/cm^2, $N_t = 10^{12}$ 1/cm^2; all other parameters remain unchanged. Red and blue arrows indicate possible energy transitions in the near-surface region under an applied DC voltage in contact with the PhiloNorm and PhiloPat compounds

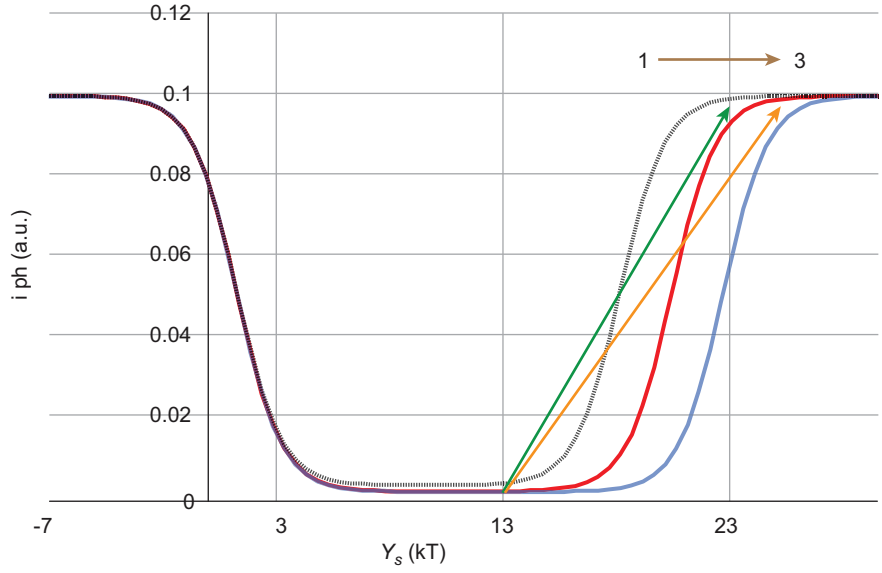

Fig. 5. Dependence of photocurrent amplitudes *i(Ys)* on the near-surface energy band bending for different ratios of charge carrier capture cross-sections: curve 1 – $c_n/c_p = 100$, curve 2 – $c_n/c_p = 10$, curve 3 – $c_n/c_p = 1$; other parameters are fixed ($N_t = 10^{12}$ cm^{-2}). Red and blue arrows indicate possible energy transitions in the near-surface region of the sensor under the influence of an applied DC voltage in contact with the PhiloNorm and PhiloPat compounds

Let us examine the effect of fast pulsed light illumination on the background of slow voltage amplitude changes. This effect is observed in both experiments with the PhiloNorm and PhiloPat compounds. It is evident in the periodic reduction of the photocurrent amplitude, which varies from relatively high values to a zero signal at the moments of maximum light intensity, as shown in **Fig. 3**. A gradual increase in voltage leads to a transition into inversion mode and also modifies the energy band bending. As a result, for a specific voltage, the energy band bending Y_s decreases to the point where the power of the parametric illumination is sufficient to fully flatten the energy bands. As can be concluded from the comparison of **Figs 3*A*** and **3*B***, complete flattening of the energy bands begins to periodically occur for PhiloPat after a higher voltage (840 mV) is applied, compared to PhiloNorm (800 mV). This pattern of amplitude change is in good agreement with the fact that a more significant negative shift occurs for PhiloNorm during the enzymatic reaction. Based on these characteristics, a second criterion for distinction can be formulated. It should be noted that with such experimental equipment, this effect is primarily due to the influence of the parametric illumination. The red and blue arrows in **Figs 4** and **5** indicate possible transitions in the near-surface region as the voltage increases for PhiloNorm and PhiloPat.

In addition to the previously proposed analysis, the sensor signals were examined as two-dimensional functions of amplitude and intensity of parametric illumination, and corresponding maps were generated. Specifically, **Figs 6*A*** and **6*B*** illustrate the difference in photocurrent before and after serum addition PhiloNorm and PhiloPat, respectively) as a function of two parameters: applied voltage and intensity of parametric illumination. This approach enables a more precise identification of the structure of photocurrent changes associated with each stage of the enzymatic chemical reaction. Consequently, the photocurrent distribution in **Fig. 6*A*** corresponds to the pathological case, while the distribution in **Fig. 6*B*** corresponds to the normal case, thereby providing a clearer representation of the changes associated with each stage of the enzymatic chemical reaction.

Fig. 6*C* is derived as the difference between the photocurrent signals defined for **Figs 6*A*** and **6*B***, with the objective of enabling visual differentiation between cases of pathological and normal ALP activity. The red and blue regions on the map in **Fig. 6*C*** represent the specific voltage and intensity ranges where the semiconductor recombination sensor can most reliably discriminate normal and pathological states. These characteristics can be attributed to the influence of additional discrete charge trapping centers at the SiO_x/Si interface, which arise from the rapid variation in parametric illumination intensity against the background of the slower voltage change. The energy levels of charge trapping accumulate non-equilibrium charge carriers over time, influencing the photocurrent amplitude, which is determined by faster recombination processes. The change in the charge state of the center occurs when the Fermi level crosses the discrete energy level of charge trapping at the surface. This behavior is observed for various applied voltage values, as illustrated in **Figs 6*A*** and **6*B***. It is likely that the energy positions and concentrations of such levels may be different; however, this case requires further investigation. Due to the complexity of the physicochemical processes involved in reactions with ALP, providing a more precise explanation of the observed effects is challenging. However, it can be asserted that the charge redistribution

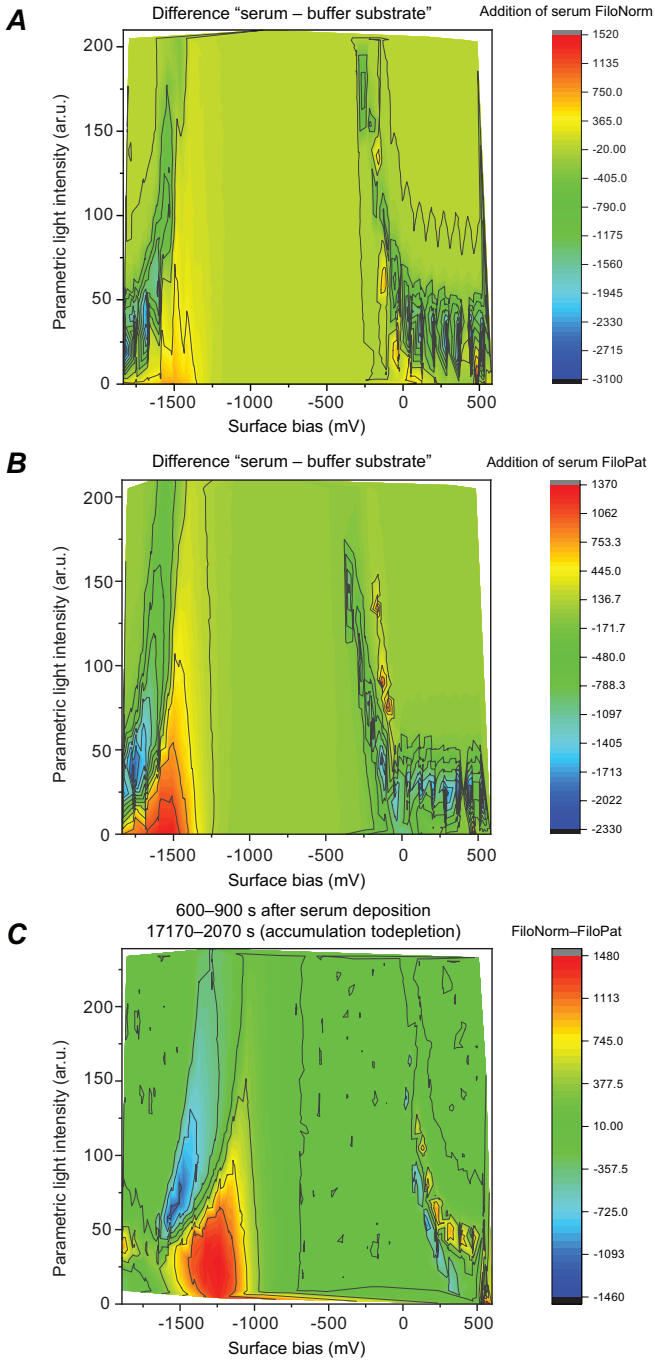

Fig. 6. Dependence of photocurrent amplitude on two variables: the amplitude of the surface bias that changes the bending of energy bands in the surface region and the intensity of parametric illumination. This is shown for the case of normal ALP activity in blood serum (***A***), pathological ALP activity in blood serum (***B***), and the differential distribution (***C***). The color gradient on the scale corresponds to the magnitude of the photocurrent

processes of reagents in chemical reactions involving ALP lead to a significant alteration of the electronic states at the SiO_x/Si interface. This contrasts with simpler cases, where the sensor's operation can be fully described by changes in surface band bending. It complicates the study of ALP activity using a semiconductor recombination sensor. However, the proposed approach allows the determination of ALP activity through an expanded set of experimental data and the analysis of the dependencies.

We can compare the biosafety characteristics of the method for determining ALP proposed by us and the reference spectroscopic method with amino-2-methyl-1-propanol-containing buffer. In both cases, the reaction substrate is *n*-nitrophenyl phosphate and the product of the biochemical reaction is *n*-nitrophenol. Therefore, both methods are equally imperfect in terms of the biosafety of the reaction product. However, the method proposed by us has the potential to reduce toxicity for laboratory personnel and environmental pollution, since it involves the use of any ALP substrates, while the reference method involves the formation of the phenolic compound itself as the product of the enzymatic reaction (since it is *n*-nitrophenyl phosphate that further reacts with 4-aminophenazone, giving a red reaction product, which is determined photometrically). Therefore, in our further studies, we intend to test the determination of ALP activity by a recombinational sensor using other, nontoxic reaction substrates (phosphoethanolamine and pyridoxal-5′-phosphate).

It should be noted that previously we successfully detected the different type of enzymes with recombinational sensor in real time (Kozynets *et al.*, 2022, 2024). The presented study not only involved the detection of ALP but also compared its activity levels in two different biological fluids. This can be regarded as another promising step towards the development of sensitive and simple method for biological fluids investigation.

The proposed structure may serve as a foundation for the development of portable, cost-effective systems for express analysis of ALP enzymatic activity. The data obtained using such systems can complement the results of more sophisticated techniques based on electrochemical and spectrophotometric analysis. Furthermore, the approach enables optical addressing and surface scanning of the sensor – where the enzymatic reactions take place – using an LED semiconductor matrix or a laser in combination with an acousto-electronic positioning system, and enables the implementation of various irradiation algorithms. This will ensure more advanced statistical processing of the photocurrent data. These factors are critical for improving detection accuracy and enhancing selectivity. Moreover, there is a reasonable expectation that the proposed method will exhibit high sensitivity, as only thin, effectively monolayer films of reagents in the cuvette are required to interact with the sensor surface. As previously noted, we intend to conduct a detailed investigation of the specific characteristics of the proposed method for ALP activity determination and to obtain its quantitative performance metrics. The objective of the present study was to demonstrate the fundamental feasibility of distinguishing between two levels of ALP activity in biological fluids using this novel approach.

CONCLUSION

The paper demonstrates the possibility of implementing a semiconductor recombination sensor for the detection of biochemical markers, specifically ALP activity in biological fluids, in real-time. The detection of ALP enzymatic activity is achieved through

specific chemical reactions catalyzed by this enzyme. These chemical reactions are accompanied by a redistribution of the reagent charges, particularly an increase in negative charge. This redistribution can be predicted based on the dissociation constant values, providing for accurate modeling of the changes in the charge states of the reagents. These changes directly influence the parameters of the recombination centers at the SiO_x/Si interface. The physical mechanism governing the operation of the proposed sensor can be explained by the Stevenson–Keyes theory, taking into account the concurrent changes in surface band bending, capture cross-sections, and recombination energy levels during molecule adsorption. The electrostatic influence mechanism is likely attributed to the recharging of centers at the SiO_x/Si interface, which leads to alterations in the interaction between reagent molecules and the sensor surface. A novel methodology for detecting ALP activity is presented, based on the use of a recombination sensor under constant voltage and parametric illumination. Additionally, a theoretical model has been developed that adequately describes the sensor's behavior under these conditions. This approach facilitates a more detailed analysis of changes in photocurrent amplitude, thereby enhancing the accuracy of ALP enzymatic activity detection and contributing to the development of new methods for studying biochemical processes.

COMPLIANCE WITH ETHICAL STANDARDS

Conflict of Interest: the authors declare that they have no conflict of interest.

Human Rights: this article does not contain any studies with human subjects performed by any of the authors.

Animal Studies: this article does not contain any studies with laboratory animals.

AUTHOR CONTRIBUTIONS

Conceptualization, [L.S.; K.O.; O.T.; S.B.]; methodology, [L.S.; K.O.; O.T.; S.B.]; research, [L.S.; K.O.; O.T.; S.B.]; resources, [L.S.; K.O.; O.T.; S.B.]; data processing, [L.S.; K.O.; O.T.; S.B.]; writing – preparation of the original project, [L.S.]; writing – review and editing, [L.S.; K.O.; O.T.; S.B.]; visualization, [K.O.] supervision, [L.S.]; project management, [L.S.; K.O.]; funding search, [–].

All authors have read and agreed to the published version of the manuscript.

REFERENCES

Atia, M. M., Mahmoud, H. A. A., Wilson, M., & Abd-Allah, E. A. (2024). A comprehensive survey of warfarin-induced hepatic toxicity using histopathological, biomarker, and molecular evaluation. *Heliyon*, 10(4), e26484. doi:10.1016/j.heliyon.2024.e26484
Crossref ● PubMed ● PMC ● Google Scholar

Azpiazu, D., Gonzalo, S., & Villa-Bellosta, R. (2019). Tissue non-specific alkaline phosphatase and vascular calcification: a potential therapeutic target. *Current Cardiology Reviews*, 15(2), 91–95. doi:10.2174/1573403x14666181031141226
Crossref ● PubMed ● PMC ● Google Scholar

Balbaied, T., & Moore, E. (2019). Overview of optical and electrochemical alkaline phosphatase (ALP) biosensors: recent approaches in cells culture techniques. *Biosensors*, 9(3), 102. doi:10.3390/bios9030102
Crossref ● PubMed ● PMC ● Google Scholar

Brichacek, A. L., & Brown, C. M. (2018). Alkaline phosphatase: a potential biomarker for stroke and implications for treatment. *Metabolic Brain Disease*, 34(1), 3–19. doi:10.1007/s11011-018-0322-3
Crossref ● PubMed ● PMC ● Google Scholar

Davis, K., Imel, E. A., & Kelley, J. (2024). Hypophosphatemic rickets and short stature. *Journal of Bone and Mineral Research*, 39(7), 821–825. doi:10.1093/jbmr/zjae103
Crossref ● PubMed ● Google Scholar

Goud, K. Y., Reddy, K. K., Khorshed, A., Kumar, V. S., Mishra, R. K., Oraby, M., Ibrahim, A. H., Kim, H., & Gobi, K. V. (2021). Electrochemical diagnostics of infectious viral diseases: trends and challenges. *Biosensors and Bioelectronics*, 180, 113112. doi:10.1016/j.bios.2021.113112
Crossref ● PubMed ● PMC ● Google Scholar

Jiang, T., Zeng, Q., & He, J. (2023). Do alkaline phosphatases have great potential in the diagnosis, prognosis, and treatment of tumors? *Translational Cancer Research*, 12(10), 2932–2945. doi:10.21037/tcr-23-1190
Crossref ● PubMed ● PMC ● Google Scholar

International Agency for Research on Cancer (IARC). (1999). Re-evaluation of some organic chemicals, hydrazine and hydrogen peroxide. In: *IARC monographs on the evaluation on the carcinogenic risks to humans* (Vol. 71, pp. 749–768). Lyon: IARC. Retrieved from https://www.ncbi.nlm.nih.gov/books/NBK499014
Google Scholar

Kalligosfyri, P. M., Miglione, A., Esposito, A., Alhardan, R., Iula, G., Atay, I., Darwish, I. A., Kurbanoglu, S., & Cinti, S. (2025). Flexible screen-printed electrochemical sensor for alkaline phosphatase detection in biofluids for biomedical applications. *ChemistryOpen*, 14(6), e202500113. doi:10.1002/open.202500113
Crossref ● PubMed ● PMC ● Google Scholar

Kaplan, L. A., Pesce, A. J., & Kazmierczak, S. C. (1996). *Clinical chemistry: theory, analysis, correlation*. Sant Louis: Mosby.
Google Scholar

Kozinetz, A. V., Tsymbalyuk, O. V., & Litvinenko, S. V. (2022). The first application of sensory structures based on photoelectric transducer for the study of enzymatic reactions. *Studia Biologica*, 16(4),3–18. doi:10.30970/sbi.1604.698
Crossref ● Google Scholar

Kozinetz, A., Sus, B., Tsymbalyuk, O., & Litvinenko, S. (2024). Photovoltaic recombination sensor as system for real-time determination of lactate dehydrogenase activity. *Sensing and Bio-Sensing Research*, 43, 100620. doi:10.1016/j.sbsr.2024.100620
Crossref ● Google Scholar

Li, Q., Wang, H., Wang, H., Deng, J., Cheng, Z., Lin, W., Zhu, R., Chen, S., Guo, J., Tang, L. V., & Hu, Y. (2023). Association between serum alkaline phosphatase levels in late pregnancy and the incidence of venous thromboembolism postpartum: a retrospective cohort study. *EClinicalMedicine*, 62, 102088. doi:10.1016/j.eclinm.2023.102088
Crossref ● PubMed ● PMC ● Google Scholar

Millán, J. L., & Whyte, M. P. (2016). Alkaline phosphatase and hypophosphatasia. *Calcified Tissue International*, 98(4), 398–416. doi:10.1007/s00223-015-0079-1
Crossref ● PubMed ● PMC ● Google Scholar

Nešvera, J., Rucká, L., & Pátek, M. (2015). Catabolism of phenol and its derivatives in bacteria: genes, their regulation, and use in the biodegradation of toxic pollutants. *Advances in Applied Microbiology*, 93, 107–160. doi:10.1016/bs.aambs.2015.06.002
Crossref ● PubMed ● Google Scholar

Pabis, A., & Kamerlin, S. C. L. (2016). Promiscuity and electrostatic flexibility in the alkaline phosphatase superfamily. *Current Opinion in Structural Biology*, 37, 14–21. doi:10.1016/j.sbi.2015.11.008
Crossref ● PubMed ● Google Scholar

Riancho, J. A. (2023). Diagnostic approach to patients with low serum alkaline phosphatase. *Calcified Tissue International*, 112(3), 289–296. doi:10.1007/s00223-022-01039-y
Crossref ● PubMed ● Google Scholar

Sato, M., Saitoh, I., Kiyokawa, Y., Iwase, Y., Kubota, N., Ibano, N., Noguchi, H., Yamasaki, Y., & Inada, E. (2021). Tissue-nonspecific alkaline phosphatase, a possible mediator of cell maturation: towards a new paradigm. *Cells*, 10(12), 3338. doi:10.3390/cells10123338
Crossref ● PubMed ● PMC ● Google Scholar

Shaban, S. M., Byeok Jo, S., Hafez, E., Ho Cho, J., & Kim, D.-H. (2022). A comprehensive overview on alkaline phosphatase targeting and reporting assays. *Coordination Chemistry Reviews*, 465, 214567. doi:10.1016/j.ccr.2022.214567
Crossref ● Google Scholar

Sharma, U., Pal, D., & Prasad, R. (2014). Alkaline phosphatase: an overview. *Indian Journal of Clinical Biochemistry*, 29(3), 269–278. doi:10.1007/s12291-013-0408-y
Crossref ● PubMed ● PMC ● Google Scholar

Si, F., Zhang, Y., Lu, J., Hou, M., Yang, H., & Liu, Y. (2023). A highly sensitive, eco-friendly electrochemical assay for alkaline phosphatase activity based on a photoATRP signal amplification strategy. *Talanta*, 252, 123775. doi:10.1016/j.talanta.2022.123775
Crossref ● PubMed ● Google Scholar

Simão, E. P., Frías, I. A. M., Andrade, C. A. S., & Oliveira, M. D. L. (2018). Nanostructured electrochemical immunosensor for detection of serological alkaline phosphatase. *Colloids and Surfaces B: Biointerfaces*, 171, 413–418. doi:10.1016/j.colsurfb.2018.07.056
Crossref ● PubMed ● Google Scholar

Su, W., Qiu, T., Zhang, M., Hao, C., Zeng, P., Huang, Z., Du, W., Yun, T., Xuan, Y., Zhang, L., Guo, Y., & Jiao, W. (2022). Systems biomarker characteristics of circulating alkaline phosphatase activities for 48 types of human diseases. *Current Medical Research and Opinion*, 38(2), 201–209. doi:10.1080/03007995.2021.2000715
Crossref ● PubMed ● Google Scholar

Tat, J., Heskett, K., Satomi, S., Pilz, R. B., Golomb, B. A., & Boss, G. R. (2021). Sodium azide poisoning: a narrative review. *Clinical Toxicology*, 59(8), 683–697. doi:10.1080/15563650.2021.1906888
Crossref ● PubMed ● PMC ● Google Scholar

Turan, S., Topcu, B., Gökce, İ., Güran, T., Atay, Z., Omar, A., Akçay, T., & Bereket, A. (2011). Serum alkaline phosphatase levels in healthy children and evaluation of alkaline phosphatase z-scores in different types of rickets. *Journal of Clinical Research in Pediatric Endocrinology*, 3(1), 7–11. doi:10.4274/jcrpe.v3i1.02
Crossref ● PubMed ● PMC ● Google Scholar

Villa-Suárez, J. M., García-Fontana, C., Andújar-Vera, F., González-Salvatierra, S., de Haro-Muñoz, T., Contreras-Bolívar, V., García-Fontana, B., & Muñoz-Torres, M. (2021). Hypophosphatasia: a unique disorder of bone mineralization. *International Journal of Molecular Sciences*, 22(9), 4303. doi:10.3390/ijms22094303
Crossref ● PubMed ● PMC ● Google Scholar

Vimalraj, S. (2020). Alkaline phosphatase: structure, expression and its function in bone mineralization. *Gene*, 754, 144855. doi:10.1016/j.gene.2020.144855
Crossref ● PubMed ● Google Scholar

Xiao, Y., Lu, J., Chang, W., Chen, Y., Li, X., Li, D., Xu, C., & Yang, H. (2019). Dynamic serum alkaline phosphatase is an indicator of overall survival in pancreatic cancer. *BMC Cancer*, 19(1), 785. doi:10.1186/s12885-019-6004-7
Crossref ● PubMed ● PMC ● Google Scholar

Young, D. S. (1997). Effects of drugs on clinical laboratory tests. *Annals of Clinical Biochemistry*, 34(6), 579–581. doi:10.1177/000456329703400601
Crossref ● PubMed ● Google Scholar

Zhang, H., Jia, Q., Piao, M., Chang, Y., Zhang, J., Tong, X., & Han, T. (2021). Screening of serum alkaline phosphatase and phosphate helps early detection of metabolic bone disease in extremely low birth weight infants. *Frontiers in Pediatrics*, 9, 642158. doi:10.3389/fped.2021.642158
Crossref ● PubMed ● PMC ● Google Scholar

ВИЯВЛЕННЯ АКТИВНОСТІ ЛУЖНОЇ ФОСФАТАЗИ В СИРОВАТЦІ КРОВІ ЗА ДОПОМОГОЮ НАПІВПРОВІДНИКОВОГО СЕНСОРА НА ОСНОВІ РЕКОМБІНАЦІЇ

Сергій Литвиненко, Олексій Козинець, Богдан Сусь, Ольга Цимбалюк

Київський національний університет імені Тараса Шевченка
вул. Володимирська, 64/13, Київ 01601, Україна

Обґрунтування. Більшість патологій організму людини (злоякісні пухлини печінки, холестаз, діабет, рак передміхурової залози та ін.) супроводжується порушенням цілісності клітин у тканинах-мішенях і виходом внутрішньоклітинних макромолекул у позаклітинне середовище. Отже, важливим діагностичним і прогностичним показником є рівень активності певних ферментів сироватки крові, які в нормі є внутрішньоклітинними. Одним із найперспективніших напрямів сучасної медичної електроніки та біофізики є розробка й оптимізація методів ферментативного скринінгу біологічних рідин. Метою дослідження є визначення активності лужної фосфатази в біологічних рідинах за допомогою рекомбінаційного сенсора на основі кремнієвої бар'єрної структури.

Матеріали та методи. Досліди проводили на препаратах стандартної сироватки крові людини. Референтне визначення активності лужної фосфатази проводили фотометрично. Проходження реакції лужної фосфатази було експериментально зареєстровано методом вимірювання фотоструму кремнієвої структури з заглибленим бар'єром в умовах впливу додаткових факторів, як-от модифіковані електричні поля або параметричне освітлення.

Результати. Досліджено біофізичні особливості визначення ензиму лужної фосфатази. Виявлення лужної фосфатази можливе внаслідок розщеплення 4-нітрофенілфосфату дофенолу, яку каталізує ензим. Означена хімічна реакція супроводжується перерозподілом зарядів реагентів (у бік збільшення негативного заряду) поблизу поверхні сенсора. Ефект детекції активності лужної фосфатази пояснюють локальним електростатичним впливом продуктів розщеплення 4-нітрофенілфосфату на параметри центрів рекомбінації поблизу поверхні кремнію, що призводить до зміни швидкості поверхневої рекомбінації та фотоструму.

Висновки. Запропонований підхід розглянуто як основу для розробки високочутливого методу виявлення та порівняння активності лужної фосфатази. Експериментально доведено, що ефективна детекція можлива завдяки перебудові електронних станів у інтерфейсі SiO_x/Si заглибленої кремнієвої бар'єрної структури після адсорбції.

Ключові слова: лужна фосфатаза, ферментативна активність, початковий вигин зон, фотоелектричний перетворювач, поверхнева швидкість рекомбінації, біомедична діагностика

Received / Одержано 31 June, 2025 | Revision / Доопрацьовано 23 July, 2025 | Accepted / Прийнято 17 September, 2025 | Published / Опубліковано 24 September, 2025